APL Photonics

RESEARCH ARTICLE | JUNE 23 2025

Spectral characterization of biphotons using quantum interferometric spectroscopy

Samuel Corona-Aquino ; Zi-Qi Zeng; Tao Xie; Shi-Xin You; Chunling Ding ; Yukun Song ; Dongzhou Wang ; Yun Meng ; Kai Zou; Xiaolong Hu ; Baihong Li ; Alfred B. U'Ren ; Roberto de J. León-Montiel ; Rui-Bo Jin

APL Photonics 10, 066118 (2025)
https://doi.org/10.1063/5.0267337

AIP Publishing

Spectral characterization of biphotons using quantum interferometric spectroscopy

Cite as: APL Photon. 10, 066118 (2025); doi: 10.1063/5.0267337
Submitted: 24 February 2025 • Accepted: 7 June 2025 •
Published Online: 23 June 2025

Samuel Corona-Aquino,[1,2,3] Zi-Qi Zeng,[3] Tao Xie,[1,3] Shi-Xin You,[3] Chunling Ding,[3] Yukun Song,[4] Dongzhou Wang,[5] Yun Meng,[6,7] Kai Zou,[6,7] Xiaolong Hu,[6,7,a)] Baihong Li,[8] Alfred B. U'Ren,[2] Roberto de J. León-Montiel,[2,a)] and Rui-Bo Jin[1,3,a)]

AFFILIATIONS

[1] Key Laboratory of Low-Dimensional Quantum Structures and Quantum Control of Ministry of Education, Department of Physics and Synergetic Innovation Center for Quantum Effects and Applications, Hunan Normal University, Changsha 410081, China
[2] Instituto de Ciencias Nucleares, Universidad Nacional Autónoma de México, Apartado Postal 70-543, 04510 CDMX, Mexico
[3] Hubei Key Laboratory of Optical Information and Pattern Recognition, Wuhan Institute of Technology, Wuhan 430205, China
[4] State Key Laboratory of Crystal Materials, Shandong University, Jinan 250100, China
[5] Jinan Institute of Quantum Technology and Hefei National Laboratory Jinan Branch, Jinan 250101, China
[6] School of Precision Instrument and Optoelectronic Engineering, Tianjin University, Tianjin 300072, China
[7] Key Laboratory of Optoelectronic Information Science and Technology, Ministry of Education, Tianjin 300072, China
[8] School of Physics and Information Science, Shaanxi University of Science and Technology, Xi'an 710021, China

[a)] **Authors to whom correspondence should be addressed:** xiaolonghu@tju.edu.cn; roberto.leon@nucleares.unam.mx; and jrbqyj@gmail.com

ABSTRACT

The spectral distribution of photon pairs produced by spontaneous parametric downconversion (SPDC) is one of the most exploited degrees of freedom in multiphoton experiments. Consequently, the characterization of such correlations is, without a doubt, a task of utmost importance. Common methods for measuring the joint spectral intensity (JSI) of correlated photon pairs often exhibit several drawbacks, such as the requirement for a bright source to offset high losses or the need for two-dimensional measurements, which can lead to prolonged acquisition times. In this work, we experimentally demonstrate a technique that allows for the reconstruction of the JSI from a single interferometric measurement, thus reducing the dimensionality of the problem. The reconstructed JSIs show good agreement with those obtained directly through a fiber spectrometer, confirming the effectiveness of our approach. This technique significantly enhances the efficiency of JSI characterization, offering a resource-efficient method for quantum state characterization in SPDC-based experiments.

INTRODUCTION

Quantum technologies have experienced accelerated development in recent years, including in areas such as quantum computing,[1,2] quantum communication,[3,4] quantum sensing,[5] and quantum metrology.[6–8] Photonic systems are particularly promising due to their scalability and stability.[9,10] One of the essential resources for these technologies is entangled photon pair generation by spontaneous parametric downconversion (SPDC),[11] which provides the necessary degrees of freedom (DoF) for a wide range of applications. Among these, the spectral distribution of photon pairs is one of the most exploited DoFs, as it is relatively simple to manage. As a result, the control and characterization of biphotonic spectral correlations, contained in the joint spectral intensity (JSI), are of vital importance in many quantum optics applications. Typically, the JSI is measured through direct spectral measurements, either by scanning with two monochromators or through the use of a fiber

spectrometer.[12,13] However, the first method is inherently inefficient since each frequency pair is probed in turn while discarding photons at other frequencies, making it impractical for low-brightness sources. The second method, although more efficient, is not suitable for spectral regions prone to losses in optical fiber and, more importantly, is unfeasible for SPDC sources with a continuous-wave (CW) pump.

A different approach to characterizing the JSI is through indirect measurements, in which spectral information can be extracted by the Fourier transformation of time (delay)-dependent interference patterns. This technique, known as quantum interferometric spectroscopy (QIS),[14,15] can be applied to any spectral region, as it does not require dispersive elements or particularly high fluxes, due to its inherently low loss nature. To date, several experimental and theoretical works have studied the QIS of biphotons. These can be grouped according to the interferometer used. The first group relies on the Hong–Ou–Mandel interferometer (HOM-I),[16] from which it is possible to obtain the frequency difference spectrum of the signal and idler photons,[15] thus making it suitable for applications in quantum imaging,[17] quantum metrology,[18] and quantum-optical coherence tomography.[19] On the other hand, to retrieve the sum-frequency spectrum of photon pairs, a possible approach is to use a QIS apparatus based on N00N state interference (N00N-SI),[20] with applications ranging from quantum microscopy[21,22] and two-photon excitation spectroscopy[23] to two-photon absorption.[24] It is worth noting that both methods yield information limited to a single dimension of the full, two-dimensional JSI.

Given that each of the QIS techniques can handle only a portion of the JSI, it is necessary to independently acquire and interpret two interferograms. This process can rapidly become impractical, as it involves different experimental configurations and time-consuming data-handling protocols. An alternative method is to use a single experimental scheme with two independent and simultaneous time delays,[29] which can be unstable and difficult to carry out experimentally. In this work, we introduce a hybrid interferometer that incorporates both the HOM-I and N00N-SI into a single delay-dependent signal. When the input two-photon state is symmetric (in the sense of invariance upon interchanging the two frequency arguments), and the JSI can be decoupled along diagonal and anti-diagonal, the complete shape of the JSI can be extracted by Fourier transforming the interferometric signals [see Fig. 1(a)]. To demonstrate the effectiveness of our interferometer, we probe two different SPDC sources in the telecom band. By comparing the retrieved spectral information with a direct, fiber-based JSI measurement, we find that the two measurements show an overlap of ~92%. This shows the potential of our low-dimensional, quantum interferometric technique in the full characterization of two-photon spectral correlations.

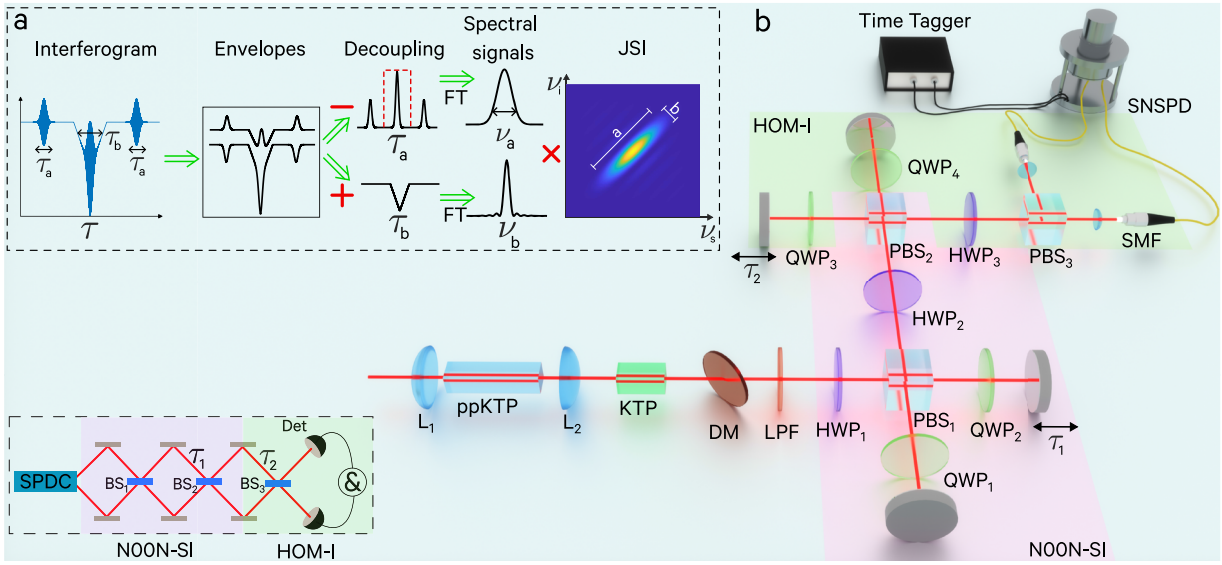

FIG. 1. Quantum interferometric spectroscopy of biphotons. (a) Schematic representation of the joint spectral intensity (JSI) reconstruction using quantum interferometric spectroscopy. The interferogram consists of characteristic temporal widths corresponding to N00N-SI (τ_a) and HOM-I (τ_b), which can be decoupled by adding or subtracting its envelopes. The JSI can then be reconstructed as the product of the Fourier-transformed decoupled signals. (b) Experimental setup of the hybrid interferometer. We generate biphotons using a type-II spontaneous parametric downconversion at telecom C-band using a ppKTP crystal. The photon pairs are then temporally matched using a KTP crystal while the pump beam is eliminated by a dichroic mirror (DM) and long-pass filters (LPFs). The combination of half-wave plates (HWPs) and polarizing beam splitters (PBSs) effectively acts as a 50:50 beam splitter, where the photon pairs are mixed to interfere.[25] To introduce time delays in a controlled manner, we use quarter-wave plates (QWPs) with mirrors in retro-reflection after PBS_1 and PBS_2.[26] Finally, at the output of PBS_3, the interfered photon pairs are collected by two single-mode fibers (SMFs). We record the experimental interferograms by performing photon counting measurements using superconducting nanowire single-photon detectors (SNSPDs)[27,28] and a time tagger. The inset shows a simplified scheme of the experimental setup.

RESULTS

Theory of complete quantum interferometric spectroscopy: The quantum state of photon pairs is mainly determined by the joint spectral amplitude (JSA), $f(\omega_s, \omega_i)$, where $\omega_{s,i}$ are the signal and idler frequencies, respectively. This function can be expressed as the product of the pump spectral envelope, $\alpha(\omega_s, \omega_i)$, and the phase-matching function, $\phi(\omega_s, \omega_i)$. In order to perform the complete spectral characterization with a single interferogram, we need to express the JSA as a separable function along the diagonal and antidiagonal directions. To do so, we introduce the change of variables, $\Omega_{s,i} = \omega_{s,i} - \omega_p/2$, where $\Omega_{s,i}$ is the spectral detuning of each photon with respect to the degenerate frequency $\omega_p/2$, where ω_p is the pump center frequency. Finally, considering $\Omega_\pm = \Omega_s \pm \Omega_i$, we can express the JSA as $f(\Omega_+, \Omega_-) = f_+(\Omega_+) f_-(\Omega_-)$, with each function depending on the sum or difference of the frequency detunings. To obtain the shape of the hybrid interferogram, let us consider that a symmetric state under frequency exchange, $f(\omega_s, \omega_i) = f(\omega_i, \omega_s)$, is sent through the interferometer shown in the inset (bottom left) of Fig. 1. The coincidence probability between the two detectors as a function of τ_1 and τ_2 is found to be[30]

$$\begin{aligned} R(\tau_1, \tau_2) = \frac{1}{2}\int_0^\infty \int_0^\infty d\Omega_+ d\Omega_- |f_+(\Omega_+)|^2 |f_-(\Omega_-)|^2 \\ \times \{1 - \frac{1}{2}\cos[(\omega_p + \Omega_+)\tau_1]\cos(\Omega_-\tau_2) - \frac{1}{2}\cos(\Omega_-\tau_2) \\ - \frac{1}{2}\cos[(\omega_p + \Omega_+)\tau_2)] + \frac{1}{4}\cos[(\omega_p + \Omega_+)(\tau_2 + \tau_1)] \\ + \frac{1}{4}\cos[(\omega_p + \Omega_+)(\tau_2 - \tau_1)]\}. \end{aligned} \tag{1}$$

Given that the second through the sixth terms in Eq. (1) have the general form of $\int_0^\infty |f_\pm(\Omega_\pm)|^2 \exp(i\Omega_\pm\tau) d\Omega_\pm$, it is possible to express the coincidence rate probability as the Fourier transform of the JSI. To explicitly show the coincidence rate of our experiment, let us consider a type-II phase-matched crystal pumped by a pulsed laser. In this scenario, the JSA will be a sinc-type phase-matching function along the Ω_- direction, multiplied by a Gaussian function along the Ω_+ direction, representing the pump spectral envelope. Therefore, considering $f(\Omega_+, \Omega_-) = \exp(-\Omega_+^2/(2\sigma_+^2))\mathrm{sinc}(\Omega_-/\sigma_-)$, the normalized coincidence counts are given by

$$\begin{aligned} R_N(\tau_1, \tau_2) = 1 - \frac{1}{2}\Lambda(\tau_2\sigma_-) - \frac{1}{2}\cos(\omega_p\tau_2) e^{-\sigma_+^2\tau_2^2} \\ + \frac{1}{4}\cos[\omega_p(\tau_2 + \tau_1)] e^{-\sigma_+^2(\tau_2+\tau_1)^2} \\ + \frac{1}{4}\cos[\omega_p(\tau_2 - \tau_1)] e^{-\sigma_+^2(\tau_2-\tau_1)^2}, \end{aligned} \tag{2}$$

where Λ is the triangular function, with zeros at $\pm 1/\sigma_-$. It is interesting to note that, in Eq. (2), the last three terms correspond to N00N-SI signals, one centered at $\tau_2 = 0$, while the other two are at $\tau_2 = \pm\tau_1$. Those signals contain fast oscillations with a period of $2\pi/\omega_p$ enveloped by Gaussian functions whose width is inversely proportional to σ_+. We remark that to fully distinguish the three different N00N-SI contributions, the condition $\tau_1 \gg 1/\sigma_+$ must be satisfied; otherwise, the signals overlap around zero delay. The second term in Eq. (2) corresponds to the typical HOM-I dip whose width is inversely proportional to σ_-.

Decoupling N00N-SI and HOM-I: Because our focus is on the diagonal and antidiagonal properties of the JSI, we can suppress the fast oscillations in the interferograms by retaining only their envelopes. To achieve this, we can eliminate the cosine terms, which is analogous to applying a short-pass frequency filter. In this way, the upper (R'_+) and lower envelopes (R'_-) may be expressed as

$$\begin{aligned} R'_\pm(\tau_1, \tau_2) = 1 \pm \frac{1}{2}e^{-\sigma_+^2\tau_2^2} - \frac{1}{2}\Lambda(\tau_2\sigma_-) \\ \pm \frac{1}{4}e^{-\sigma_+^2(\tau_2+\tau_1)^2} \pm \frac{1}{4}e^{-\sigma_+^2(\tau_2-\tau_1)^2}. \end{aligned} \tag{3}$$

With a proper combination of $R'_+(\tau_1, \tau_2)$ and $R'_-(\tau_1, \tau_2)$, we can find an expression containing information exclusively relating to the HOM-I as follows:

$$R'_+ + R'_- = 2 - \Lambda(\tau_2\sigma_-). \tag{4}$$

Similarly, a signal related exclusively to the N00N-SI can be written as

$$R'_+ - R'_- = e^{-\sigma_+^2\tau_2^2} + \frac{1}{2}e^{-\sigma_+^2(\tau_2+\tau_1)^2} + \frac{1}{2}e^{-\sigma_+^2(\tau_2-\tau_1)^2}. \tag{5}$$

Because each term in Eq. (5) provides identical information about the N00N-SI, differing only in the position along the delay axis, we can suppress the side distributions by applying a rectangular filter. Consequently, when performing the Fourier transform of $R'_+ - R'_-$, we obtain the pump spectral envelope, whereas the Fourier transform of $R'_+ + R'_-$ yields the phase-matching function. Finally, the JSI can be reconstructed as the product of these two functions, showing that it is possible to characterize the two-photon state from a single interferometric signal.

Measuring the hybrid interferogram: We now proceed to present the experimental characterization of two different SPDC sources using our technique. For this purpose, we make use of the experimental setup shown in Fig. 1(b). The experimental details can be found in the section titled Methods. Note that while our theoretical derivations use angular frequencies, $\omega_{s,i}$, it is convenient to use linear frequencies, $\nu_{s,i} = \omega_{s,i}/2\pi$, to display the results with the greatest clarity. The experimentally obtained interferograms are shown in blue solid lines in Figs. 2(a) and 2(d). These correspond to the positively correlated and uncorrelated sources, respectively. In these plots, we can identify the different terms depicted in Eq. (2). First, we can observe three N00N-SI contributions; two of them are centered at $\tau_2 = \pm 4$ ps, with a third one centered at $\tau_2 = 0$ ps. Note that the typical HOM-I dip for a type-II source appears at $\tau_2 = 0$, with a visibility close to 90%. Both signals can be clearly distinguished in the case of the correlated source because the N00N-SI signal is narrower than the HOM-I dip, while for the uncorrelated source, the signals show a larger degree of overlap. To decouple the HOM-I from the N00N-SI signal, we compute the interferogram envelopes via spline interpolation. The results are shown as black dashed lines in panels (a) and (d) of Fig. 2. Then, by fitting those curves to Eq. (3), it is straightforward to find the upper and lower envelopes, which are presented as red dashed lines and solid yellow lines, respectively. Finally, we add and subtract these envelopes, as described by Eqs. (4) and (5), to separate the interferometric signals. For the positively correlated source, the obtained N00N-SI information is shown in Fig. 2(b), while the corresponding HOM-I information is displayed in panel (c)

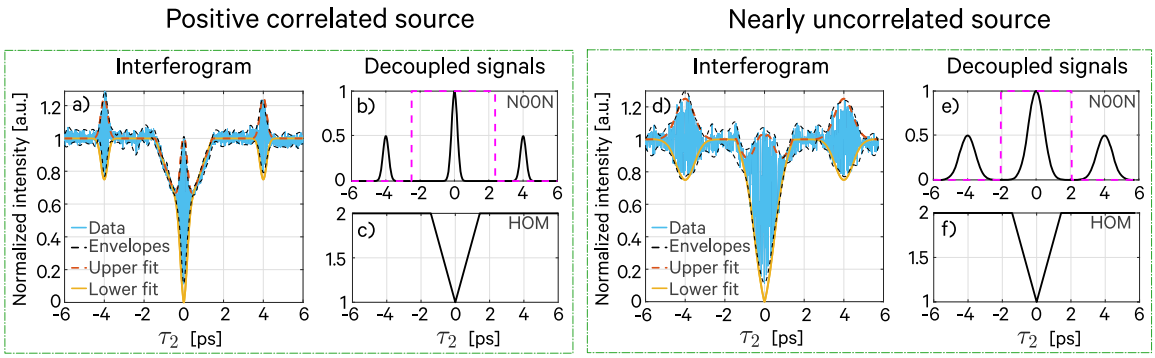

FIG. 2. Hybrid interferogram and component-decoupling process. The green left-hand box presents the results for the positively correlated source, while the right-hand one shows the results for the nearly uncorrelated case. Panels (a) and (d) show the hybrid interferogram (blue solid line), where three N00N-SI signals are observed: two at $\tau_2 = \pm\tau_1$ and one at $\tau_2 = 0$. The latter is superimposed on a HOM-I dip. The black dashed lines show the upper (R'_+) and lower (R'_-) envelopes calculated from a spline interpolation. The red dashed lines and yellow solid lines show the fit to Eq. (3) of those envelopes. The second column in each box depicts the decoupled signals for each interferogram. Panels (b) and (e) show the triple N00N-SI signal (black solid line). Because each of the three signals contains the same information, the side peaks are removed by using a rectangular filter, drawn with a magenta dashed line. Finally, panels (c) and (f) show the HOM-I dip obtained as the sum of the envelopes $R'_+ + R'_-$. Note that the widths of the HOM-I dips in both rows are equivalent. This occurs because both sources were produced with the same crystal.

of the same figure. For the uncorrelated case, the information for the N00N-SI and the HOM-I is presented in Fig. 2(e) and 2(f), respectively.

To obtain the pump spectral envelope in each case, we crop the side lobes of the signals displayed in Figs. 2(b) and 2(e) before applying the Fourier transform. The rect function used to crop them is indicated with a magenta dashed line. A similar procedure is done to the HOM-I information shown in Figs. 2(c) and 2(f) by subtracting the offset value. The results of such transformations can be seen in the first row of Fig. 3. Panels (a) and (e) correspond to Gaussian functions representing the pump spectral envelope for the positively correlated and uncorrelated sources, respectively. The phase-matching function is found to be a sinc^2 signal [shown in panels (b) and (f)] for both the positively correlated and the uncorrelated source. As one might expect, the pump spectral envelope is wider than the phase-matching function for the positively correlated source, while for the uncorrelated case, they are of comparable width. In addition, since the same crystal was used for both sources (see the section titled Methods), one anticipates observing similar HOM-I signals for both sources. This is confirmed by the results shown in panels 3(b) and 3(f). Finally, by using the distributions shown in the first row of Fig. 3, we can reconstruct the JSI. The resulting spectral distributions for the positively correlated and uncorrelated sources are shown in panels (a) and (c) of Fig. 4, respectively.

Direct measurement of the JSI: To verify the correct performance of our hybrid interferometer, we carried out a direct measurement of the JSI by means of a fiber spectrometer. The direct-measurement results for the positively correlated and uncorrelated sources are shown in Figs. 4(b) and 4(d), respectively. One can retrieve the pump spectral envelope and phase-matching functions from these signals by making a projection on the diagonal and anti-diagonal axes. This process results in the plots shown in the second row of Fig. 3. In all cases, the normalized data are shown as a blue dotted line, while the fit to a Gaussian distribution (for the pump spectral shape) or a sinc^2 function (for the phase-matching function) is presented as a solid red line. For the sake of comparison, we have included the full width at half maximum (FWHM) of all plots. We note that the pump distribution obtained by directly measuring the JSI is slightly smaller than that obtained with our technique. These differences can mainly be attributed to slight asymmetries in the JSI, as observed in the case of Fig. 4(d). Note that the two-photon source described in Fig. 4(d) is produced by reducing the spectral width of the Ti:Sa laser using an interference filter. This results in a slightly asymmetric Gaussian pump. By comparing Figs. 4(c) and 4(d), we can clearly see that, because of the way it is designed, our method symmetrizes the JSI. This ultimately leads to discrepancies between methods. Another possible source of error is that when projecting the measured JSI [see Fig. 4(b)] the counts at the edges along the antidiagonal are not sufficient. Therefore, a longer measurement would be required to obtain adequate statistics and avoid underestimating the width along the diagonals. On the other hand, the widths of the phase matching functions recovered with our proposed method closely match those recovered through a direct measurement. This highlights the effectiveness of our technique in scenarios for which direct JSI measurement is not possible.

DISCUSSION

Our proposed technique enables the complete characterization of the JSI of an unknown two-photon source in a single, one-dimensional measurement. This is managed by subjecting the probed light to the combined effects of HOM-I and N00N-SI interferometers in a single apparatus. While such interferometers have been used separately for QIS, their combined effect enables the simultaneous retrieval of all the information in the JSI. This is because both the HOM-I and N00N-SI interferometers, being single-parameter interferometers, can only access a single projection of the JSI. In this work, we have shown that, although we implemented a two-parameter interferometer, τ_1 and τ_2, scanning

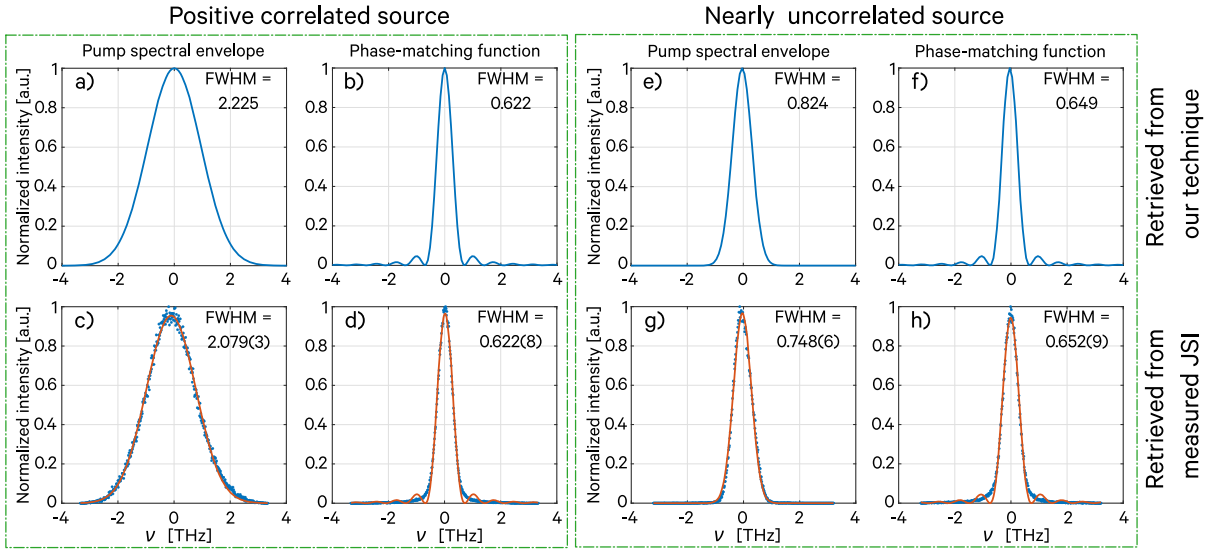

FIG. 3. Pump envelope and phase-matching function reconstruction. The green left-hand box shows the results for the positively correlated source, while the green right-hand box shows the results for the uncorrelated case. The first row displays the results via our technique, whereas the second row presents the results from the directly measured JSI. Pump envelopes, represented as Gaussian functions shown in panels (a) and (e), are the result of Fourier transforming the signals shown in Figs. 2(b) and 2(e), respectively. The sinc^2 functions shown in panels (b) and (f) were obtained by taking the Fourier transform of the HOM-I dips shown in Figs. 2(c) and 2(f), respectively. For the results shown in the second row, blue dotted lines are the projections obtained from the measured JSI, while the red curve is the fit. The anti-diagonal projection [panels (c) and (g)] represents the pump envelope, while the phase-matching function [panels (d) and (h)] results from projection along the diagonal direction.

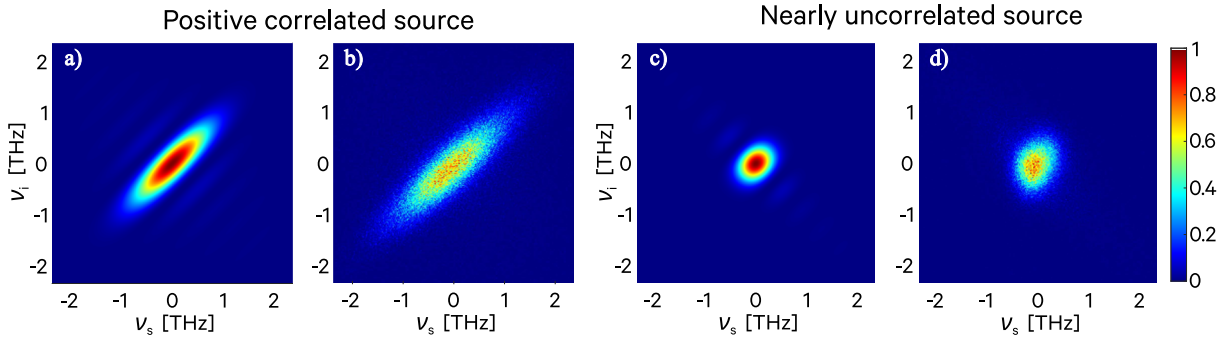

FIG. 4. Reconstructed and directly measured JSI. Reconstructed JSI using our hybrid interferometer for (a) positively correlated and (c) nearly uncorrelated photons. The phase-matching function and pump spectral shape, from which the JSIs are reconstructed, can be seen in the first row of Fig. 3. To assess the performance of our technique, we made use of a fiber spectrometer to directly measure the JSI of both sources. The results are shown in panels (b) and (d). The overlap between the JSIs is found to be ~92% for both sources, thus showing the effectiveness of our low-dimensional technique.

only one of them is sufficient to access the entire spectral information. This approach allows for greater information retrieval while maintaining the setup's manageability. It is worth noting that our method involves measuring a time-dependent signal, a considerable simplification compared to standard spectral characterization based on monochromators and spectrometers. As can be noted, the main assumption of our method is the symmetric structure of the JSI. Given that this technique is based on projection along the main diagonals, a direct generalization for characterizing asymmetric sources falls outside of its scope. However, we point out that the technique itself provides indications when dealing with an asymmetric source. More specifically, as the two-photon state becomes asymmetric, the visibilities of the interferograms decrease. If this behavior is identified in the interferograms, it is still possible to reconstruct the JSI using an auxiliary measurement, namely, the single-photon spectrum, which is easier to perform than measuring the joint spectrum directly. By having three different projections, it is possible to reconstruct the principal widths and the orientation of the JSI, assuming an arbitrarily oriented elliptical shape. To provide an overview of the achievable spectral resolution, let us consider its applicability

to ultra-broadband sources. In such sources, the spectral bandwidth typically spans from tens to hundreds of THz, depending on the central wavelength. For such broad bandwidths, the interferogram duration is on the order of femtoseconds, thus meaning that a piezoelectric stage may provide sufficient resolution to sample displacements below 12 μm. This represents an advantage over fiber spectrometers since the fiber dispersion changes significantly for broadband sources. Similarly, monochromator-based methods require adjustments to the diffraction gratings depending on the spectral range. On the other hand, for narrowband sources, our method can achieve resolutions down to 0.02 nm for sources around 800 nm and 0.08 nm for sources at the telecom band. These bandwidths correspond to a few GHz and require a motor travel of ~1.5 cm to recover the corresponding interferogram, which lasts several tens of picoseconds. This spectral resolution is already comparable to what can be obtained using a monochromator coupled to single-mode fibers. Finally, since our method relies on photon counting, one can achieve high signal-to-noise ratios (SNRs). This allows for cleaner interferograms that ultimately lead to the efficient calculation of envelopes and the reconstruction of the sought-after JSI distribution.

CONCLUSION

In summary, we have experimentally demonstrated a technique for the spectral characterization of biphotons based on quantum interferometric measurements. By decoupling different contributions from HOM- and N00N-like interferometric signals, we are able to extract the pump's spectral envelope and the phase-matching function of two-photon states, thus enabling the efficient reconstruction of the JSI. The proposed method is robust, easy to operate, and free from spectral limitations, which makes it applicable to bandwidths ranging from tens of THz to tens of GHz. It is particularly useful for sources where the photon flux is too low for traditional spectral measurement techniques characterized by high losses, such as scanning monochromators. It can also be used with SPDC sources pumped by CW light, which are incompatible with fiber spectrometers. In addition, we point out that our proposed method is readily compatible with machine-learning techniques, which ensures its applicability in the context of emerging smart photonic sensors.[31–33] Although this method is limited to sources with frequency exchange symmetry, our results have proven to be robust and reliable, with an overlap larger than 92% with the directly measured JSI distributions. Moreover, by reducing the measuring process from two-dimensional (in frequency) to one-dimensional (in time), this indirect method is inherently faster than other techniques, limited only by the scanning speed of the linear motor. Beyond the time gain, it is important to mention that this method allows for the simultaneous characterization of all the information in the JSI. In this way, unlike other QIS methods where changes to the experimental setup are required to switch from one interferometer to another, we can ensure that the acquisition conditions remain identical.

METHODS

In our experiment, we make use of a pulsed laser operating at 775 nm (with a 76 MHz repetition rate) to pump the crystal, phase-matched for a type-II SPDC process. For both sources—namely, positively correlated and nearly uncorrelated photons—we use the same nonlinear crystal with different pump bandwidths. For the first case, the laser is centered at 775 nm with a FWHM of 4.65 nm, generating the positive correlation shown in Figs. 4(a) and 4(b). Conversely, in the second case, the pump is filtered to obtain a FWHM of 2.96 nm, generating a JSI with almost zero correlation, as evidenced in the results shown in Figs. 4(c) and 4(d). The beam is focused through a 100 mm-focal length lens (L1), ensuring a beam waist, w_0, of 50 μm. The ppKTP crystal has a length of 10-mm and a period of 46.2 μm; its temperature can be controlled by an oven, and it is centered on the focal plane of lens L1.

To collimate the downconverted light, a plano–convex lens (L2) is situated at a distance of f_2 = 100 mm from the center of the nonlinear crystal. Subsequently, a dichroic mirror (DM) designed to reflect wavelengths $\lambda < 1100$ nm, in conjunction with a long-pass filter (IF), effectively suppresses the remaining pump photons. This allows only those wavelengths $\lambda > 1200$ nm to be transmitted. The photon pairs traverse a 5 mm KTP crystal to compensate for the group velocity difference, ensuring temporal overlap at the exit face. Photon pairs then encounter a half-wave plate (HWP_1) with its fast axis oriented at 22.5° relative to the horizontal, which, together with a polarizing beam splitter (PBS_1), effectively acts as a non-polarizing beam splitter. After the splitting process, a controllable delay (τ_1) is introduced, and the pairs are recombined using a system comprising $QWP_{1,2}$ (fast axis oriented at 45° relative to the horizontal) and a reflection mirror in each arm. In our experiments, this delay was fixed at $\tau_1 = 4$ ps to fulfill the condition $\tau_1 \gg 1/\sigma_+$ so that we may fully distinguish the three separate N00N-SI contributions.

The collinear photons emerging from PBS_1, still with orthogonal polarizations, undergo non-deterministic splitting. This is done by a half-wave plate (HWP_2) with its fast axis oriented at 22.5° relative to the horizontal, followed by a polarizing beam splitter (PBS_2). Up to this point in the experiment, the combination of two effective BSs (composed of HWPs and PBSs) with a time delay between them acts as a N00N state interferometer. If two detectors are placed at the output arms of PBS_2, the usual signal associated with a N00N-SI is obtained.

To complete our hybrid interferometer, we introduce a second delay, τ_2. This is achieved through a system similar to the one described above, which incorporates quarter-wave plates ($QWP_{3,4}$) with their axes oriented at 45° relative to the horizontal and a mirror for retroreflection in each path. In this case, the relative delay is managed by placing one mirror on a stepper motor with a minimum step of 1 μm. After the τ_2 delay, photon pairs undergo further splitting via a polarizing beam splitter in combination with a half-wave plate (HWP3) with its axis oriented at 22.5° from the horizontal. This scheme results in a similar setup to a typical HOM-I interferometer, in which the pairs with orthogonal polarizations and a relative delay between them arrive at the same port of the BS. Finally, the resulting paths are coupled into a single-mode fiber (SMF) connected to superconducting nanowire single-photon detectors (SNSPDs), with its output signals temporally tagged (TT) to obtain single and double counts on a PC. The exposure time is set to one second. Our proposed method is based on interference effects, and as such, it exhibits the typical stability (or lack thereof) associated with interferometers. However, it is worth pointing out that the key

element of our technique is the extraction of the envelope of the interferograms. Given that standard schemes such as HOM-I and N00N-SI are used, the stability of a tabletop experiment is sufficient to ensure the reliability of our strategy. As a reference, to verify the stability of the setup, we performed a long interferogram measurement. During a 40-min data-acquisition session, the signal remained stable.

ACKNOWLEDGMENTS

The authors thank Professor Chenglong You for the helpful discussions. This work was supported by the National Natural Science Foundation of China (Grant Nos. 92365106, 12074299, and 12074309), by the Natural Science Foundation of Hubei Province (Grant No. 2022CFA039), by the Innovation Program for Quantum Science and Technology (Grant Nos. 2021ZD0300800 and 2024ZD0301000), and the Scientific Research Program Funded by Shaanxi Provincial Education Department (Program No. 24JR034). R.J.L.-M. thankfully acknowledges the financial support by DGAPA-UNAM under Project No. UNAM-PAPIIT IN101623.

AUTHOR DECLARATIONS

Conflict of Interest

The authors have no conflicts to disclose.

Author Contributions

The experiment was designed by S.C.A., Z.-Q.Z., and R.-B.J. The theoretical description was developed by S.C.A., B.L., and R.-B.J. The experiment was performed by S.C.A., Z.-Q.Z., T.X., S.-X.Y., and C.D. The data were analyzed by S.C.A., Z.-Q.Z., and R.-B.J. The ppKTP crystals were supplied by Y.S. and D.W. The SNSPDs were supplied and assembled by Y.M., K.Z., and X.H. The project was supervised by A.B.U., R.J.L.M., and R.-B.J. The idea was conceived by B.L. and R.-B.J. All authors contributed to the writing of this paper and approved the final version of this paper.

Samuel Corona-Aquino: Data curation (equal); Formal analysis (equal); Investigation (equal); Methodology (equal); Validation (equal); Writing – original draft (equal); Writing – review & editing (equal). **Zi-Qi Zeng**: Data curation (equal); Investigation (equal); Methodology (equal); Validation (equal); Writing – original draft (equal); Writing – review & editing (equal). **Tao Xie**: Investigation (equal); Methodology (equal); Writing – original draft (equal); Writing – review & editing (equal). **Shi-Xin You**: Investigation (equal); Methodology (equal); Writing – original draft (equal); Writing – review & editing (equal). **Chunling Ding**: Investigation (equal); Methodology (equal); Writing – original draft (equal); Writing – review & editing (equal). **Yukun Song**: Resources (equal); Writing – original draft (equal); Writing – review & editing (equal). **Dongzhou Wang**: Funding acquisition (equal); Resources (equal); Writing – original draft (equal); Writing – review & editing (equal). **Yun Meng**: Resources (equal); Writing – original draft (equal); Writing – review & editing (equal). **Kai Zou**: Resources (equal); Writing – original draft (equal); Writing – review & editing (equal). **Xiaolong Hu**: Resources (equal); Writing – original draft (equal); Writing – review & editing (equal). **Baihong Li**: Conceptualization (equal); Formal analysis (equal); Validation (equal); Writing – original draft (equal); Writing – review & editing (equal) **Alfred B. U'Ren**: Supervision (equal); Validation (equal); Writing – original draft (equal); Writing – review & editing (equal). **Roberto de J. León-Montiel**: Funding acquisition (equal); Supervision (equal); Validation (equal); Writing – original draft (equal); Writing – review & editing (equal). **Rui-Bo Jin**: Conceptualization (equal); Data curation (equal); Formal analysis (equal); Funding acquisition (equal); Project administration (equal); Supervision (equal); Writing – original draft (equal); Writing – review & editing (equal).

DATA AVAILABILITY

The data that support the findings of this study are available from the corresponding author upon reasonable request.

REFERENCES

[1] B. P. Lanyon, M. Barbieri, M. P. Almeida, T. Jennewein, T. C. Ralph, K. J. Resch, G. J. Pryde, J. L. O'Brien, A. Gilchrist, and A. G. White, Nat. Phys. **5**, 134 (2009).
[2] P. Kok, W. J. Munro, K. Nemoto, T. C. Ralph, J. P. Dowling, and G. J. Milburn, Rev. Mod. Phys. **79**, 135 (2007).
[3] T. Zhong, F. N. C. Wong, A. Restelli, and J. C. Bienfang, Opt. Express **20**, 26868 (2012).
[4] J. M. Lukens and P. Lougovski, Optica **4**, 8 (2017).
[5] N. Thomas-Peter, B. J. Smith, A. Datta, L. Zhang, U. Dorner, and I. A. Walmsley, Phys. Rev. Lett. **107**, 113603 (2011).
[6] I. Afek, O. Ambar, and Y. Silberberg, Science **328**, 879 (2010).
[7] V. Giovannetti, S. Lloyd, and L. Maccone, Nat. Photonics **5**, 222 (2011).
[8] Y. Chen, L. Hong, and L. Chen, Front. Phys. **10**, 892519 (2022).
[9] W. Luo, L. Cao, Y. Shi, L. Wan, H. Zhang, S. Li, G. Chen, Y. Li, S. Li, Y. Wang, S. Sun, M. F. Karim, H. Cai, L. C. Kwek, and A. Q. Liu, Light Sci. Appl. **12**, 175 (2023).
[10] R.-B. Jin, Z.-Q. Zeng, C. You, and C. Yuan, Prog. Quantum Electron. **96**, 100519 (2024).
[11] Z. Zeng, S. You, Z. Yang, C. Yuan, C. You, and R. Jin, Chin. Opt. Lett. **22**, 021901 (2024).
[12] K. Zielnicki, K. Garay-Palmett, D. Cruz-Delgado, H. Cruz-Ramirez, M. F. O'Boyle, B. Fang, V. O. Lorenz, A. B. U'Ren, P. G. Kwiat, and J. Mod, J. Mod. Opt. **65**, 1141 (2018).
[13] R.-B. Jin, Z.-Q. Zeng, D. Xu, C.-Z. Yuan, B.-H. Li, Y. Wang, R. Shimizu, M. Takeoka, M. Fujiwara, M. Sasaki, and P.-X. Lu, Sci. China: Phys., Mech. Astron. **67**, 250312 (2024).
[14] R.-B. Jin and R. Shimizu, Optica **5**, 93 (2018).
[15] H. Seki, K. Miyajima, and R. Shimizu, Phys. Rev. A **106**, 063716 (2022).
[16] C. K. Hong, Z. Y. Ou, and L. Mandel, Phys. Rev. Lett. **59**, 2044 (1987).
[17] N. Mohan, O. Minaeva, G. N. Goltsman, M. F. Saleh, M. B. Nasr, A. V. Sergienko, B. E. Saleh, and M. C. Teich, Appl. Opt. **48**, 4009 (2009).
[18] A. Lyons, G. C. Knee, E. Bolduc, T. Roger, J. Leach, E. M. Gauger, and D. Faccio, Sci. Adv. **4**, eaap9416 (2018).
[19] P. Y. Graciano, A. M. A. Martínez, D. Lopez-Mago, G. Castro-Olvera, M. Rosete-Aguilar, J. Garduño-Mejía, R. R. Alarcón, H. C. Ramírez, and A. B. U'Ren, Sci. Rep. **9**, 8954 (2019).
[20] A. N. Boto, P. Kok, D. S. Abrams, S. L. Braunstein, C. P. Williams, and J. P. Dowling, Phys. Rev. Lett. **85**, 2733 (2000).
[21] T. Ono, R. Okamoto, and S. Takeuchi, Nat. Commun. **4**, 2426 (2013).

[22]Y. Israel, S. Rosen, and Y. Silberberg, Phys. Rev. Lett. **112**, 103604 (2014).
[23]Y. Chen, R. de J León-Montiel, and L. Chen, New J. Phys. **24**, 113014 (2022).
[24]Á. Martínez-Tapia, S. Corona-Aquino, F. Triana-Arango, C. You, R.-B. Jin, O. S. Magaña-Loaiza, S.-H. Dong, A. B. U'Ren, and R. de J. León-Montiel, APL Photonics **8**, 036104 (2023).
[25]N. S. Bisht and R. Shimizu, J. Opt. Soc. Am. B **32**, 550 (2015).
[26]J. C. Bird, F. Liang, B. H. Solheim, and G. G. Shepherd, Meas. Sci. Technol. **6**, 1368 (1995).
[27]X. Chi, K. Zou, C. Gu, J. Zichi, Y. Cheng, N. Hu, X. Lan, S. Chen, Z. Lin, V. Zwiller, and X. Hu, Opt. Lett. **43**, 5017 (2018).
[28]Y. Meng, K. Zou, N. Hu, L. Xu, X. Lan, S. Steinhauer, S. Gyger, V. Zwiller, and X. Hu, ACS Photonics **9**, 1547 (2022).
[29]A. F. Abouraddy, T. M. Yarnall, and G. Di Giuseppe, Phys. Rev. A **87**, 062106 (2013).
[30]B. Li, C. Chen, X. Xiang, R. Quan, R. Dong, S. Zhang, X. Hao, and R.-B. Jin, Phys. Rev. A **108**, 023713 (2023).
[31]A. Herrero-Bermello, J. Li, M. Khazaei, Y. Grinberg, A. V. Velasco, M. Vachon, P. Cheben, L. Stankovic, V. Stankovic, D.-X. Xu, J. H. Schmid, and C. Alonso-Ramos, Opt. Lett. **44**, 5840 (2019).
[32]Á. Martínez-Tapia and R. de J. León-Montiel, AVS Quantum Sci. **7**, 021401 (2025).
[33]J. D. Huerta-Morales, C. You, O. S. Magaña-Loaiza, S.-H. Dong, R. de J. León-Montiel, and M. A. Quiroz-Juárez, "Smart machine vision for universal spatial-mode reconstruction," IEEE Trans. Neural Networks Learn. Syst. (published online 2025).